

Object Tracking by a Robot Manipulator: A Robust Cooperative Visual Servoing Approach*

W. E. Dixon¹, E. Zergeroglu², Y. Fang³, and D. M. Dawson³

¹Engineering Science and Technology Division – Robotics,
Oak Ridge National Laboratory, P.O. Box 2008, Oak Ridge, TN 37831-6305

²Lucent Technologies, Bell Lab Innovations Optical Fiber Solutions, 50 Halls Rd, Sturbridge MA, 01566

³Department of Electrical and Computer Engineering, Clemson University, Clemson, SC 29634-0915

“The submitted manuscript has been authored by a contractor of the U.S. Government under contract DE-AC05-00OR22725. Accordingly, the U.S. Government retains a nonexclusive, royalty-free license to publish or reproduce the published form of this contribution, or allow others to do so, for U.S. Government purposes.”

To appear in the *IEEE International Conference on Robotics and Automation*,
May 11-15, 2002, Washington, D.C.

Keywords: Visual Servoing, Adaptive Control, and Nonlinear Lyapunov-Based Control

E-mail: dixonwe@ornl.gov, Telephone: (865)574-9025

* This research was supported in part by the Eugene P. Wigner Fellowship Program of the Oak Ridge National Laboratory (ORNL), managed by UT-Battelle, LLC, for the U.S. Department of Energy (DOE) under contract DE-AC05-00OR22725 and in part by the U.S. DOE Environmental Management Sciences Program (EMSP) projects ID No. 82797 and ID No. 82794 at ORNL, by ONR Project No. N00014-00-F-0485 at ORNL, and by U.S. NSF Grants DMI-9457967, DMI-9813213, EPS-9630167, ONR Grant N00014-99-1-0589, a DOC Grant, and an ARO Automotive Center Grant.

Object Tracking by a Robot Manipulator: A Robust Cooperative Visual Servoing Approach

W. E. Dixon[†], E. Zergeroglu[‡], Y. Fang[§], and D. M. Dawson[§]

[†]Engineering Science and Technology Div.-Robotics, Oak Ridge National Laboratory, Oak Ridge, TN, 37831-6305

[‡]Lucent Technologies, Bell Lab Innovations Optical Fiber Solutions, 50 Halls Rd, Sturbridge MA, 01566

[§]Department of Electrical & Computer Engineering, Clemson University, Clemson, SC 29634-0915

email: dixonwe@ornl.gov; ezerger@lucent.com; yfang, ddawson@ces.clemson.edu

Abstract: In this paper, we utilize a Lyapunov-based design approach to construct a visual servoing controller for a robot manipulator that ensures uniformly ultimately bounded (UUB) end-effector position tracking performance despite parametric uncertainty throughout the entire robot/camera system. The UUB end-effector tracking result exploits information from both a fixed camera and a camera-in-hand, although both cameras contain parametric uncertainty in the calibration parameters (e.g., focal length, image center, scaling factors, and camera position and orientation). The advantages of the cooperative camera configuration are that: (i) the fixed camera can be mounted so that a large robot workspace is visible, (ii) the camera-in hand is mounted so that a high resolution, close-up view of an object is achieved, facilitating the potential for more precise robotic motion, and (iii) the fixed camera provides a mechanism for treating the problem of determining the relative velocity of the robot end-effector with respect to the object for the camera-in-hand object tracking problem when the camera is uncalibrated.

I. INTRODUCTION

To enable robotic systems with the ability to operate autonomously in unstructured environments, researchers have investigated the use of vision-based approaches (see [10], [26], and the references within for a survey of these techniques). Although a vision system can provide a robot with a unique sense of perception, several technical issues have impacted the design of robust visual servo robot controllers including¹: (i) camera configuration (pixel resolution versus field-of-view), (ii) camera calibration, and (iii) dynamic effects of the robotic system. For example, for vision systems that utilize a camera mounted in a fixed configuration (i.e., the eye-to-hand configuration), the camera is typically mounted far enough away from the robot workspace to ensure that the robot and desired target objects will remain in the camera's view. Unfortunately, by mounting the camera in this configuration the task-space area that corresponds to a pixel in the image-space can be quite large, resulting in low resolution and noisy position measurements; hence, the precision and stability of the robot could be adversely affected. For vision systems that utilize a camera mounted in the camera-in-hand configuration (also referred to as the eye-in-hand configuration), the camera is naturally close to the workspace, providing for higher resolution measurements and less noise due to the fact that each pixel represents a smaller task-space area; however, the field-of-view of the camera is significantly reduced (i.e., an object may be located in the robot's workspace but be out of the camera's view due to the position of the end-effector). Recently, Flandin et al. [8] proposed an innovative multi-camera solution to address the aforementioned configuration issues. Specifically, [8] made the first steps towards cooperatively utilizing global and local information obtained from a fixed camera and a camera-in-hand; unfortunately, to prove the stability results, the translation and rotation tasks of the controller were treated separately (i.e., the coupling terms were ignored) and the cameras were considered to be calibrated. The

This research was supported in part by the Eugene P. Wigner Fellowship Program of the Oak Ridge National Laboratory (ORNL), managed by UT-Battelle, LLC, for the U.S. Department of Energy (DOE) under contract DE-AC05-00OR22725 and in part by the U.S. DOE Environmental Management Sciences Program (EMSP) projects ID No. 82797 and ID No. 82794 at ORNL, by ONR Project No. N00014-00-F-0485 at ORNL, and by U.S. NSF Grant DMI-9457967, ONR Grant N00014-99-1-0589, a DOC Grant, and an ARO Automotive Center Grant.

¹Note that delays due to image processing has historically been a problem related to the development of visual servo controllers; however, as camera and computation advances continue to be made, this issue is becoming less important.

approach by Flandin et al. is in contrast to typical multi-camera approaches, that utilize a stereo-based configuration (e.g., [1], [2], [11], [12], [13], [14], [23], [29]), since stereo-based approaches typically do not simultaneously exploit local and global views of the robot and the workspace.

A problem common to both the fixed camera and the camera-in-hand configuration is the need for the cameras to be calibrated. That is, if the intrinsic and extrinsic camera calibration parameters² are unknown, or slowly change over time, then the relationship between the task-space and the image-space will be erroneous, leading to unpredictable robotic performance and instability. As stated in [4], [11], [15], another issue that has impacted the development of robust vision-based controllers is that few visual-servo controllers have been proposed that take into account the nonlinear robot dynamics. Motivated by the desire to take into account uncalibrated camera effects and the mechanical dynamics of the robot, several researchers have recently designed visual-servo controllers that ensure the convergence of the position error for the setpoint regulation problem. For example, Kelly and Marquez [17] designed a setpoint controller for the fixed-camera problem that compensated for unknown intrinsic camera parameters, provided perfect knowledge of the camera orientation was available. In [15], Kelly redesigned the setpoint controller of [17] to also take into account uncertainties associated with the camera orientation; however, the controller yielded a local asymptotic stability result that required exact knowledge of the robot gravitational term and that the difference between the estimated and actual camera orientation be restricted to the interval $(-90^\circ, 90^\circ)$. In [16], Kelly et al. extended the transpose Jacobian control philosophy given in [30] to develop a position regulation controller for the camera-in-hand problem, provided exact knowledge of the robot gravitational term is available and that depth information was measurable. In [24], Maruyama and Fujita proposed position setpoint controllers for the camera-in-hand configuration; however, the proposed controllers required exact knowledge of the camera orientation and assumed equal camera scaling factors. In [32], Zergeroglu et al. proposed a uniformly ultimately bounded (UUB) regulating controller for the camera-in-hand configuration provided the camera orientation is within a certain range.

In addition to the setpoint regulation problem, several results have also been proposed for the tracking problem. For example, in [3], Bishop and Spong developed an adaptive visual servo position tracking control scheme for the fixed camera configuration that compensated for camera calibration errors in the feedback loop; however, the result required exact knowledge of the robot dynamics and that the desired position trajectory be persistently exciting. In [18], Kelly et al. utilized a composite velocity inner loop, image-based outer loop position tracking controller for the fixed camera configuration to obtain a local asymptotic stability result; however, exact model knowledge of the robot dynamics and a calibrated camera are required, and the difference between the estimated and actual camera orientation is restricted to the interval $(-90^\circ, 90^\circ)$. In [32], Zergeroglu et al. also proposed a UUB position tracking controller that rejects uncertainty throughout the entire robot-camera system for a fixed camera configuration. Recently, in [31], Zergeroglu et al. designed an adaptive position tracking controller for a fixed camera configuration that accounted for parametric uncertainty throughout the entire robot-camera system provided the camera orientation is restricted to the interval $(-90^\circ, 90^\circ)$. Note that due to the relative velocity problem associated with the camera-in-hand configuration, all of the previ-

²The camera calibration parameters are composed of the intrinsic parameters (i.e., image center, camera scale factors, and camera magnification factor) and extrinsic parameters (i.e., camera position and orientation).

ously mentioned tracking results are developed for the fixed camera configuration. That is, for the camera-in-hand configuration, camera calibration is further necessitated by the need to relate the velocities between the camera and the image-space objects.

Inspired by the recent results given in [8], in this paper we consider a new cooperative visual servoing approach that utilizes information from both a fixed camera and a camera-in-hand. The advantages of the cooperative camera configuration are that: (i) the fixed camera can be mounted so that the complete robot workspace is visible, (ii) the camera-in-hand is mounted so that a high resolution, close-up view of an object is achieved, facilitating the potential for more precise robotic motion, and (iii) the fixed camera provides a mechanism for treating the problem of determining the relative velocity of the robot end-effector with respect to the object for the uncalibrated camera-in-hand tracking problem. Specifically, using Lyapunov-based design and analysis techniques similar to [32], we construct a robust nonlinear visual servoing controller that forces the end-effector of a robot manipulator to achieve UUB tracking of an object trajectory that is represented by an uncertain object motion model, provided the initial orientation of the camera-in-hand is within a certain range. To provide for greater robustness, we simultaneously confront the issues of parametric uncertainty in the camera calibration and in the parameters of the dynamic model of the robot manipulator (e.g., mass, inertia, friction coefficients, and additive bounded disturbances). In comparison to previous work, we note that the visual servo control result in this paper has several advantages over previous results such as: (i) the more general problem of object tracking is confronted versus setpoint regulation, (ii) it is the first visual servo result that exploits information obtained from an uncalibrated camera-in-hand configuration to allow the end-effector of a robot manipulator to track a moving object (i.e., the novel cooperative camera approach provides a mechanism to overcome the relative velocity issue described previously), and (iii) the UUB tracking result is obtained despite parametric uncertainty in the robot dynamics (which includes unmodeled additive bounded disturbances) and parametric uncertainty in the camera calibration.

This paper is organized in the following manner. In Section II, we develop the dynamic model of a 2-link planar robot manipulator, the pin hole lens models for both the fixed camera and the camera-in-hand configurations, and the object motion model. In the Section III, we develop the robust visual servo tracking control design and in Section IV, we prove that the controller yields UUB tracking. Simulation results are presented in Section V to illustrate the closed-loop performance of the developed controller. Concluding remarks are given in Section VI.

II. MODEL DEVELOPMENT

A. Robot Dynamic Model

The dynamic model for a two-link, planar robot manipulator is given as follows [22]

$$M(q)\ddot{q} + V_m(q, \dot{q})\dot{q} + G(q) + F(\dot{q}) + T_d = \tau \quad (1)$$

where $q(t)$, $\dot{q}(t)$, $\ddot{q}(t) \in \mathbb{R}^2$ denote the link position, velocity, and acceleration vectors, respectively, $M(q) \in \mathbb{R}^{2 \times 2}$ represents the inertia matrix, $V_m(q, \dot{q}) \in \mathbb{R}^{2 \times 2}$ represents centripetal-Coriolis matrix, $G(q) \in \mathbb{R}^2$ denotes the gravity effects, $F(\dot{q}) \in \mathbb{R}^2$ represents the friction effects, $T_d \in \mathbb{R}^2$ denotes a vector of unknown additive bounded disturbances, and $\tau(t) \in \mathbb{R}^2$ is the torque input vector. The robot model of (1) satisfies the following properties [22] that are utilized in the subsequent control design and analysis.

Property 1: The inertia matrix $M(q)$ is symmetric and positive-definite, and satisfies the following inequalities

$$m_1 \|\xi\|^2 \leq \xi^T M(q) \xi \leq m_2 \|\xi\|^2 \quad \forall \xi \in \mathbb{R}^2 \quad (2)$$

where $m_1, m_2 \in \mathbb{R}$ are positive bounding constants and $\|\cdot\|$ denotes the standard Euclidean norm.

Property 2: The inertia and centripetal-Coriolis matrices satisfy the following skew symmetric relationship

$$\xi^T \left(\frac{1}{2} \dot{M}(q) - V_m(q, \dot{q}) \right) \xi = 0 \quad \forall \xi \in \mathbb{R}^2 \quad (3)$$

where $\dot{M}(q)$ denotes the time derivative of the inertia matrix.

Property 3: The left side of (1) can be partially linearly parameterized as shown below

$$M(q)\ddot{q} + V_m(q, \dot{q})\dot{q} + G(q) + F(\dot{q}) = W(q, \dot{q}, \ddot{q}) \phi \quad (4)$$

where $\phi \in \mathbb{R}^m$ contains the constant system parameters, and the regression matrix $W(\cdot) \in \mathbb{R}^{2 \times m}$ contains known functions dependent on the signals $q(t)$, $\dot{q}(t)$, and $\ddot{q}(t)$.

With regard to the kinematic structure of the robot manipulator, we make the following assumptions.

Assumption 1: There is a set of task-space variables $x \in \mathbb{R}^2$, an open set $S_1 \subset \mathbb{R}^2$, and a function $\Omega \in C^2(S_1)$, $\Omega : S_1 \rightarrow \mathbb{R}^2$, such that

$$x = \Omega(q) \quad (5)$$

denotes the forward kinematics and

$$J(q) = \frac{\partial \Omega(q)}{\partial q} \in \mathbb{R}^{2 \times 2} \quad (6)$$

represents the Jacobian matrix where $J \in C^1(S_1)$.

Assumption 2: The minimum singular value of $J(q)$, is greater than a known, small positive constant $\delta > 0$, such that $\max \{\|J^{-1}(q)\|\}$ is known a priori, and hence, all kinematic singularities are always avoided. Moreover, the Jacobian is upper bounded as follows

$$\|J\| \leq \zeta_J \quad (7)$$

where $\zeta_J \in \mathbb{R}^1$ is a known bounding constant.

Remark 1: For simplicity, the previous model development has been formulated for a non-redundant robot manipulator (i.e., we assume $n = 2$); however, the results delineated in this paper can be extended to the redundant case (see [31] for details).

B. Camera Model

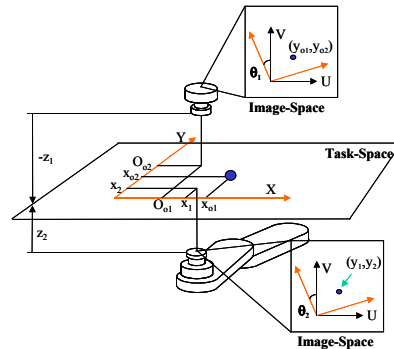


Fig. 1. Cooperative camera configuration

The camera-robot configuration that is considered in this paper is shown in Figure 1. As shown in Figure 1, we exploit the use of both a fixed camera and a camera-in-hand. To model each of the cameras, we utilize the so-called pinhole lens model. Specifically, the model for the fixed camera is given below [3]

$$\begin{bmatrix} y_{o1} \\ y_{o2} \end{bmatrix} = -B_1 \begin{bmatrix} x_{o1} \\ x_{o2} \end{bmatrix} + p \quad (8)$$

where $y_o(t) = [y_{o1}(t) \ y_{o2}(t)]^T \in \mathbb{R}^2$ represents the image-space position of an object, $x_o(t) = [x_{o1}(t) \ x_{o2}(t)]^T \in \mathbb{R}^2$ represents the task-space position of an object, $p \in \mathbb{R}^2$ is a constant vector defined as follows

$$p = \begin{bmatrix} O_1 \\ O_2 \end{bmatrix} + B_1 \begin{bmatrix} O_{o1} \\ O_{o2} \end{bmatrix}, \quad (9)$$

where $[O_1, O_2]^T \in \mathbb{R}^2$ denotes the image center that is defined as the frame buffer coordinates of the intersection of the optical axis with the image plane (see [21] for details), $[O_{o1}, O_{o2}]^T \in \mathbb{R}^2$ denotes the projection of the camera's optical center on the task-space, and $B_1 \in \mathbb{R}^{2 \times 2}$ denotes a subsequently defined constant scaled rotation matrix. The model for the camera-in-hand is given below [24]

$$\begin{bmatrix} y_1 \\ y_2 \end{bmatrix} = B_2 \left(\begin{bmatrix} x_1 \\ x_2 \end{bmatrix} - \begin{bmatrix} x_{o1} \\ x_{o2} \end{bmatrix} \right) \quad (10)$$

where $y(t) = [y_1(t) \ y_2(t)]^T \in \mathbb{R}^2$ represents the image-space position of an object, $x(t) = [x_1(t) \ x_2(t)]^T \in \mathbb{R}^2$ represents the

task-space position of the end-effector, $x_o(t)$ is given in (8), and $B_2(q) \in R^{2 \times 2}$ denotes a scaled rotation matrix. The scaled rotation matrices B_1 and $B_2(q)$ given in (8), (9), and (10), are defined as follows

$$B_i = A_i R_i \quad \forall i = 1, 2 \quad (11)$$

where $A_i \in R^{2 \times 2}$ denotes a diagonal, positive-definite, constant matrix defined as follows

$$A_i = \begin{bmatrix} \alpha_{i1} & 0 \\ 0 & \alpha_{i2} \end{bmatrix} \quad \forall i = 1, 2 \quad (12)$$

where $\alpha_{i1}, \alpha_{i2} \in R^1$ are positive constants defined as follows

$$\alpha_{i1} = \beta_{i1} \frac{\lambda_i}{z_i} \quad \alpha_{i2} = \beta_{i2} \frac{\lambda_i}{z_i} \quad \forall i = 1, 2 \quad (13)$$

where $\beta_{i1}, \beta_{i2} \in R^1$ denote unknown constant scale factors (in pixels/m) for the i -th camera, $\lambda_i \in R^1$ denotes the constant unknown focal length of the i -th camera, $z_i \in R^1$ represents the constant unknown distance from the i -th camera's optical center to the task-space plane, and $R_i(\cdot) \in R^{2 \times 2}$ is a rotation matrix defined as

$$R_i(\cdot) = \begin{bmatrix} \cos(\cdot) & \sin(\cdot) \\ -\sin(\cdot) & \cos(\cdot) \end{bmatrix}. \quad (14)$$

The counterclockwise rotation angle of the image-space coordinate system with respect to the task-space coordinate system, denoted by $\theta \in R^1$, is defined as follows for the fixed camera configuration

$$\theta = \theta_1 \quad (15)$$

where $\theta_1 \in R^1$ denotes a constant unknown angle, and is defined as follows for the camera-in-hand configuration

$$\theta(t) = \theta_2 + \sum_{i=1}^2 q_i(t) \quad (16)$$

where $q_i(t)$ denotes the position of the i -th link of the robot manipulator and $\theta_2 \in R^1$ is the unknown constant angle between the end-effector and the camera-in-hand. Hence, the overall rotation matrix for the camera-in-hand configuration can be written in the following form

$$R_2(\theta) = R_2 \left(\theta_2 + \sum_{i=1}^2 q_i \right) = R_2(\theta_2) R_2(q_1, q_2). \quad (17)$$

Property 4: The following constant scaled rotation matrix $\bar{B} \in R^{2 \times 2}$

$$\bar{B} = A_2 R_2(\theta_2) \quad (18)$$

where A_2 and $R_2(\theta_2)$ were defined in (12), (14), and (17), satisfies the following property

$$\zeta^T \bar{B} \zeta = \zeta^T \left(\frac{\bar{B} + \bar{B}^T}{2} \right) \zeta \quad \forall \zeta \in R^2. \quad (19)$$

Provided the following inequality is valid

$$\cos(\theta_2) > \left| \frac{\beta_{21} - \beta_{22}}{\beta_{21} + \beta_{22}} \right| \quad (20)$$

where $\theta_2, \beta_{21}, \beta_{22}$ are given in (13) and (16), the symmetric matrix $\bar{B} + \bar{B}^T$ will be positive-definite (proof available upon request).

Assumption 3: Both the fixed camera and the camera-in-hand are assumed to be mounted such that the image plane of each camera is parallel to each other and to the robot's plane of motion, and that images can be captured by both cameras throughout the entire robot workspace.

Assumption 4: The task-space position of an object, denoted in (8) as $x_o(t)$, is assumed to remain in the view of the cameras, and the image-space trajectory of the object is assumed to be bounded (i.e., $y_o(t), \dot{y}_o(t) \in L_\infty$).

Assumption 5: The absolute value of the unknown camera parameters $\alpha_1, \alpha_2, O_1, O_2, O_{o1}, O_{o2}$ are assumed to be bounded by known positive bounding constants.

Remark 2: With respect to (20), note that

$$0 \leq \left| \frac{\beta_{21} - \beta_{22}}{\beta_{21} + \beta_{22}} \right| < 1, \quad (21)$$

and that the condition on θ_2 can be written as $\theta_2 \in \{-|\theta_c|, |\theta_c|\}$ where θ_c is determined from a given set of values for β_{21} and β_{22} . If the camera's scale factors have the same value (i.e., $\beta_{21} = \beta_{22}$), then $\theta_c = 90^\circ$. As the difference between the values of β_{21} and β_{22} increases, the ratio $\left| \frac{\beta_{21} - \beta_{22}}{\beta_{21} + \beta_{22}} \right| \rightarrow 1$, and hence, $\theta_c \rightarrow 0^\circ$. Since in most camera systems β_{21} and β_{22} are similar values (i.e., $\left| \frac{\beta_{21} - \beta_{22}}{\beta_{21} + \beta_{22}} \right| \ll 1$, and hence, $\theta_c \gg 0^\circ$), the condition given in (20) is not difficult to satisfy in practice. Further note that no restrictions are placed on the parameters of the fixed camera.

Remark 3: Note that the camera configuration illustrated in Figure 1 is motivated by the desire to eliminate the possibility of the robot end-effector occluding the object from the fixed camera. If knowledge of the object's geometry were given a priori and the object was larger than the robot end-effector, then both the fixed camera and the camera-in-hand could be mounted above the object. Also note that if the potential for end-effector occlusion of the object is eliminated by the aforementioned geometrical issues, a fixed camera solution could be developed as an extension to the results given in [31]; however, the advantages of using the camera-in-hand (e.g., higher resolution measurement that may result in greater robotic precision) would be lost.

C. Object Motion Model

The task-space trajectory can be represented by an object motion model [9]. For example, the object position and its time derivative for a straight line, circle, and the so-called "Figure 8" trajectories are given as follows [9]

$$\left. \begin{aligned} \begin{bmatrix} x_{o1} \\ x_{o2} \end{bmatrix} &= \begin{bmatrix} x_{o1} \\ x_{o2} \end{bmatrix} \\ \begin{bmatrix} \dot{x}_{o1} \\ \dot{x}_{o2} \end{bmatrix} &= \begin{bmatrix} v_{x1} \\ v_{x2} \end{bmatrix} \end{aligned} \right\} \text{Straight Line} \quad (22)$$

$$\left. \begin{aligned} \begin{bmatrix} x_{o1} \\ x_{o2} \end{bmatrix} &= \begin{bmatrix} r_1 \cos(\omega t) + c_x \\ r_1 \sin(\omega t) + c_y \end{bmatrix} \\ \begin{bmatrix} \dot{x}_{o1} \\ \dot{x}_{o2} \end{bmatrix} &= \begin{bmatrix} -x_{o2} \omega + \omega c_y \\ x_{o1} \omega - \omega c_x \end{bmatrix} \end{aligned} \right\} \text{Circle} \quad (23)$$

$$\left. \begin{aligned} \begin{bmatrix} x_{o1} \\ x_{o2} \end{bmatrix} &= \begin{bmatrix} r_1 \cos(\omega t) \\ r_2 \sin(2\omega t) \end{bmatrix} \\ \begin{bmatrix} \dot{x}_{o1} \\ \dot{x}_{o2} \end{bmatrix} &= \begin{bmatrix} -\frac{r_1^2 \omega}{2r_2} \frac{x_{o2}}{x_{o1}} \\ \frac{2r_2 \omega}{r_1^2} x_{o2} - \frac{r_1^2 \omega}{2r_2} \frac{x_{o2}^2}{x_{o1}^2} \end{bmatrix} \end{aligned} \right\} \text{Figure 8} \quad (24)$$

where $v_{x1}, v_{x2} \in R^1$ denote the constant, unknown linear velocity of the object, $r_1, r_2, c_x, c_y \in R^1$ are positive unknown constants, and $\omega \in R^1$ denotes the constant, unknown angular velocity of the object. With regard to the object motion model, the following assumption is made.

Assumption 6: The absolute value of the object motion parameters (e.g., $v_{x1}, v_{x2}, \omega, r_1, r_2, c_x, c_y$) are assumed to be upper bounded by known, positive constants.

Motivated by the desire to rewrite $\dot{x}_o(t)$ in terms of measurable signals, we multiply (8) by $-B_1^{-1}$ and then rearrange the resulting expression as follows

$$\begin{bmatrix} x_{o1} \\ x_{o2} \end{bmatrix} = -B_1^{-1} \left(\begin{bmatrix} y_{o1} \\ y_{o2} \end{bmatrix} - p \right). \quad (25)$$

After substituting (25) into (22), (23), and (24) and utilizing Assumptions 5 and 6, an upper bound for $\dot{x}_o(t)$ can be formulated as follows

$$\|\dot{x}_o(t)\| \leq \rho_1(y_o) + \rho_2 \quad (26)$$

where $\rho_1(y_o) \in R^1$ is a known, positive bounding term dependant on $y_o(t)$, and $\rho_2 \in R^1$ is a known, positive constant bounding term.

III. CONTROL DEVELOPMENT

The control objective for this paper is to force the end-effector of a robot manipulator to track the time-varying position of an object. To quantify this objective, we define the task-space position tracking error $e(t) \in R^2$ as follows

$$e = x - x_o \quad (27)$$

where $x_o(t)$ and $x(t)$ are given in (8) and (10), respectively. After taking the time derivative of (27), the following expression can be obtained

$$\dot{e} = J\dot{q} - \dot{x}_o \quad (28)$$

where (5) and (6) have been utilized. After some algebraic manipulation, (28) can be rewritten as follows

$$\dot{e} = -J\eta - \dot{x}_o + Ju \quad (29)$$

where $\eta(t) \in R^2$ is defined as

$$\eta = u - \dot{q} \quad (30)$$

and $u(t) \in R^2$ is an auxiliary control signal. Based on the open-loop error system for $e(t)$ given in (29) and the subsequent stability analysis, we design the control signal $u(t)$ as follows

$$u = -J^{-1} \left(k_c + k_{n1} (\rho_1(y_o) + \rho_2)^2 \right) R_2^T(q_1, q_2) y \quad (31)$$

where $k_c, k_{n1} \in R^1$ are positive constant control gains, $R_2(q_1, q_2)$ was defined in (17), and $\rho_1(y_o)$ and ρ_2 were given in (26). After substituting (31) into (29) for $u(t)$, the following expression is obtained

$$\begin{aligned} \dot{e} &= -J\eta - \dot{x}_o - \left(k_c + k_{n1} (\rho_1(y_o) + \rho_2)^2 \right) \\ &\quad \cdot R_2^T(q_1, q_2) \bar{B} R_2(q_1, q_2) e \end{aligned} \quad (32)$$

where (10), (11), (17), (18), and (27) were utilized.

To determine the closed-loop error system for $\eta(t)$, we take the time derivative of (30) and premultiply the resulting expression by $M(q)$ as follows

$$M\dot{\eta} = Y\phi - V_m\eta + T_d - \tau \quad (33)$$

where (1) and (30) were utilized and the linear parameterization $Y(u, \dot{u}, t)\phi$ is defined as follows

$$Y\phi = M\dot{u} + V_mu + G + F \quad (34)$$

where $Y(u, \dot{u}, t) \in R^{2 \times p}$ denotes a measurable regression matrix and $\phi \in R^p$ denotes a vector of unknown constant parameters. Based on the expression given in (33) and the subsequent stability analysis, we design the control torque input as follows

$$\tau = Y\hat{\phi} + k\eta + k_{n2}\zeta_2^2\eta + \frac{\rho_3^2\eta}{\rho_3\|\eta\| + \varepsilon} \quad (35)$$

where $\hat{\phi}$ is a constant best-guess estimate of the constant unknown parameters given in ϕ , where $k, k_{n2}, \varepsilon \in R^1$ are positive constant control gains, and $\rho_3(u, \dot{u}, t) \in R^1$ is a known positive bounding function that is defined as follows

$$\rho_3 \geq \|Y\hat{\phi}\| + \|T_d\| \quad (36)$$

where $\tilde{\phi} \in R^p$ denotes the mismatch between the constant unknown parameters and the constant best-guess estimate as shown below

$$\tilde{\phi} = \phi - \hat{\phi}. \quad (37)$$

After substituting (35) into (33) for $\tau(t)$, we obtain the closed-loop error system for $\eta(t)$ as follows

$$M\dot{\eta} = -V_m\eta + Y\tilde{\phi} + T_d - k\eta - \frac{\rho_3^2\eta}{\rho_3\|\eta\| + \varepsilon} - k_{n2}\zeta_2^2\eta. \quad (38)$$

Remark 4: Based on the fact that $\hat{\phi}$ is a constant best-guess estimate of the constant unknown parameters given in ϕ , it is clear that $\tilde{\phi} \in L_\infty \forall t$.

Remark 5: For the special case of the straight line motion described by (22), $\dot{x}_o(t)$ is independent of $y_o(t)$, and hence, the bound given in (26) simplifies to the following inequality

$$\|\dot{x}_o(t)\| \leq \rho_2. \quad (39)$$

Based on the control input given in (31) and (35) and the modified bound given in (39), it is evident that information from the fixed

camera is not utilized, and hence, the object tracking problem can be solved using only the camera-in-hand for this special case.

Remark 6: If an object motion model is not available, then the open-loop dynamics for $e(t)$ given in (29) can be written as follows

$$\dot{e} = -J\eta + B_1^{-1}\dot{y}_o + Ju \quad (40)$$

where the time derivative of (25) has been utilized. Based on the open-loop error dynamics given in (40), the control input $u(t)$ given in (31) can be redesigned as follows

$$u = -J^{-1} \left(k_c + k_{n1} (\zeta_B \dot{y}_o)^2 \right) R_2^T(q_1, q_2) y \quad (41)$$

where $\zeta_B \in R^1$ is a positive bounding constant defined as follows

$$\|B_1^{-1}\| \leq \zeta_B. \quad (42)$$

The controller given in (35) and (41) would result in exactly the same stability result that would be obtained using (31), (35), and the object motion model; however, since the controller given in (41) is dependant on $\dot{y}_o(t)$, it is clear from (34) and (35) that $Y_2(u, \dot{u}, t)$ and $\tau(t)$ would require that $\ddot{y}_o(t)$ be measurable. Hence, by exploiting an object motion model, the requirement for $\ddot{y}_o(t)$ to be measurable is eliminated.

IV. STABILITY ANALYSIS

Theorem 7: Provided that the camera space parameters satisfy the inequality given in (20), UUB position tracking is achieved in the sense that

$$\|e(t)\| \leq \sqrt{\frac{\lambda_2}{\lambda_1} \|\Psi(0)\|^2 \exp\left(-\frac{\lambda_2}{\lambda_2} t\right) + \frac{\lambda_4 \lambda_2}{\lambda_3 \lambda_1} \left(1 - \exp\left(-\frac{\lambda_2}{\lambda_2} t\right)\right)} \quad (43)$$

where $\Psi(t) \in R^4$ is defined as follows

$$\Psi \triangleq \begin{bmatrix} e^T & \eta^T \end{bmatrix}^T \quad (44)$$

and $\lambda_1, \lambda_2, \lambda_3, \lambda_4 \in R^1$ are positive bounding constants defined as

$$\begin{aligned} \lambda_1 &= \frac{1}{2} \min\{1, m_1\}, & \lambda_2 &= \frac{1}{2} \max\{1, m_2\}, \\ \lambda_3 &= \min\left\{k, k_c \gamma_B - \frac{1}{4k_{n2}}\right\}, & \lambda_4 &= \left(\varepsilon + \frac{1}{4k_{n1} \gamma_B}\right) \end{aligned} \quad (45)$$

where m_1 and m_2 are given in (2), k_c, k_{n1} are given in (31), k, k_{n2} and ε are given in (35), and $\gamma_B \in R^1$ is a positive bounding constant defined as

$$\gamma_B = \lambda_{\min} \left\{ \frac{\bar{B} + \bar{B}^T}{2} \right\} > 0, \quad (46)$$

where \bar{B} was defined in (18), and $\lambda_{\min}\{\cdot\}$ denotes the minimum eigenvalue of a matrix. To ensure that λ_3 is positive, k_c and k_{n2} must be selected to ensure that the following inequality is satisfied

$$4k_c k_{n2} > \frac{1}{\gamma_B}. \quad (47)$$

Proof: To prove Theorem 7, we define a non-negative function $V(t) \in R^1$ as follows

$$V = \frac{1}{2} e^T e + \frac{1}{2} \eta^T M \eta, \quad (48)$$

which can be lower and upper bounded according to the following inequalities

$$\lambda_1 \|\Psi\|^2 \leq V \leq \lambda_2 \|\Psi\|^2 \quad (49)$$

where $\Psi(t)$, λ_1 , and λ_2 were defined in (44) and (45). After taking the time derivative of (48) and substituting (32) and (38) into the resulting expression, we obtain the following expression

$$\begin{aligned} \dot{V} &= - \left(k_c + k_{n1} (\rho_1(y_o) + \rho_2)^2 \right) \\ &\quad \cdot \left[e^T R_2^T(q_1, q_2) \left(\frac{\bar{B} + \bar{B}^T}{2} \right) R_2(q_1, q_2) e \right] - e^T J \eta \\ &\quad - e^T \dot{x}_o - k \eta^T \eta + \eta^T (Y\tilde{\phi} + T_d - \frac{\rho_3^2\eta}{\rho_3\|\eta\| + \varepsilon} - k_{n2}\zeta_2^2\eta) \end{aligned} \quad (50)$$

where (3) and (19) were utilized. Based on the fact that $\bar{B} + \bar{B}^T$ is positive-definite and symmetric, we can invoke the Raleigh-Ritz

Theorem [22], to develop a lower bound for the bracketed term of (50) as follows

$$\gamma_B \|e\|^2 \leq e^T R_2^T (q_1, q_2) \left(\frac{\bar{B} + \bar{B}^T}{2} \right) R_2 (q_1, q_2) e \quad (51)$$

where the fact that

$$\|R_2 (q_1, q_2) e\|^2 = \|e\|^2$$

was utilized, and γ_B was defined in (46). After utilizing (7) and (36), an upper bound for (50) can be developed as follows

$$\begin{aligned} \dot{V} \leq & -k_c \gamma_B \|e\|^2 - k \|\eta\|^2 + [\zeta_J \|e\| \|\eta\| \\ & - k_{n2} \zeta_J^2 \|\eta\|^2] + \left[\rho_3 \|\eta\| - \frac{\rho_3^2 \|\eta\|^2}{\rho_3 \|\eta\| + \varepsilon} \right] \\ & + \left[\|e\| \|\dot{x}_o\| - k_{n1} \gamma_B (\rho_1 (y_o) + \rho_2)^2 \|e\|^2 \right]. \end{aligned} \quad (52)$$

After completing the squares on the bracketed terms in (52), we can formulate the following upper bound

$$\dot{V} \leq - \left(k_c \gamma_B - \frac{1}{4k_{n2}} \right) \|e\|^2 - k \|\eta\|^2 + \varepsilon + \frac{1}{4k_{n1} \gamma_B}. \quad (53)$$

Provided the gain condition given in (47) is satisfied, we can develop an upper bound for (53) as follows

$$\dot{V} \leq -\lambda_3 \|\Psi\|^2 + \lambda_4 \quad (54)$$

where $\Psi(t)$, λ_3 , and λ_4 were defined in (44) and (45). From the upper bound on $V(t)$ given in (49), we can further upper bound $\dot{V}(t)$ as shown below

$$\dot{V} \leq -\frac{\lambda_3}{\lambda_2} V + \lambda_4. \quad (55)$$

The differential inequality of (55) can now be solved to yield the following expression

$$V(t) \leq V(0) \exp\left(-\frac{\lambda_3}{\lambda_2} t\right) + \frac{\lambda_4 \lambda_2}{\lambda_3} \left(1 - \exp\left(-\frac{\lambda_3}{\lambda_2} t\right)\right). \quad (56)$$

Given (48) and (56), it is clear from (44) that $\Psi(t)$, $e(t)$, $\eta(t) \in L_\infty$. Based on the fact that $e(t) \in L_\infty$, we can utilize (10-17) and (27) to prove that $y(t) \in L_\infty$; hence, from (31), and the assumption that $y_o(t) \in L_\infty$, we can conclude that $u(t) \in L_\infty$. Based on the assumption that $\dot{y}_o(t) \in L_\infty$ and the fact that $e(t)$, $\eta(t)$, $u(t) \in L_\infty$, we can utilize (29) and (30) to prove that $\dot{e}(t)$, $\dot{q}(t) \in L_\infty$. Note that since $q(t)$ only appears in the camera model and control development as the argument of bounded trigonometric functions, we cannot show that $q(t) \in L_\infty$; however, all signals in the manipulator kinematics/dynamics and the control remain bounded independent of the boundedness of $q(t)$. Based on the fact that $\dot{e}(t)$, $\dot{q}(t) \in L_\infty$, we can take the time derivative of (10) to prove that $\dot{y}(t) \in L_\infty$; hence, by taking the time derivative of (31) and utilizing Assumption 1 and the assumption that $\dot{y}_o(t) \in L_\infty$, we can now prove that $\dot{u}(t)$, $Y(u, \dot{u}, t)$, $\tau(t) \in L_\infty$. Based on the fact that all the closed-loop signals remain bounded, we can now utilize (49), to formulate an upper bound for $\Psi(t)$ as follows

$$\|\Psi(t)\| \leq \sqrt{\frac{\lambda_2}{\lambda_1} \|\Psi(0)\|^2 \exp\left(-\frac{\lambda_3}{\lambda_2} t\right) + \frac{\lambda_4 \lambda_2}{\lambda_3 \lambda_1} \left(1 - \exp\left(-\frac{\lambda_3}{\lambda_2} t\right)\right)}. \quad (57)$$

Based on (44) and (57), we can prove that the end-effector position tracking error $e(t)$ can be bounded by the expression given in (43). \square

V. SIMULATION RESULTS

The controller developed in the previous section was simulated based on the following image space (for the fixed camera) trajectory

$$\begin{bmatrix} y_{o1} \\ y_{o2} \end{bmatrix} = \begin{bmatrix} 16 + 10 \sin(0.1t) \\ 14 + 10 \cos(0.1t) \end{bmatrix}. \quad (58)$$

The camera-in-hand and fixed cameras that were utilized to view the object system are modeled by (8-17) with the following parameters

$$\begin{aligned} O_{o1} &= 0.2 \text{ m}, & O_{o2} &= 0.1 \text{ m}, & O_1 &= O_2 = 0 \text{ m}, \\ \beta_{ij} &= 1024, & \lambda_i &= 0.08 \text{ m}, & \forall i, j &= 1, 2 \\ z_1 &= 1.2 \text{ m}, & z_2 &= 3.0 \text{ m}, & \theta_1 &= 30 \text{ deg}, & \theta_2 &= 10 \text{ deg} \end{aligned} \quad (59)$$

The task-space end-effector position and velocity for the fixed and the in-hand camera were initialized as follows

$$x(0) = [0.4618, 0.4398]^T \text{ m} \quad \dot{x}(0) = [0, 0]^T \text{ m/sec.} \quad (60)$$

The camera-in-hand was simulated using the dynamics for a two-link, direct-drive, horizontally-planar, Integrated Motion Inc. manipulator.

After tuning the controller given in (31) and (35) the following control gains were selected

$$k_{s1} = 10.0, \quad k_{s2} = 22.5, \quad \rho = 5, \quad \varepsilon = 0.02$$

where $k_{s1}, k_{s2} \in R^1$ are defined as follows

$$k_{s1} \geq k_c + k_{n1} (\zeta_B \zeta_y)^2 \quad k_{s2} \geq k + k_{n2} \zeta_J^2 \quad (61)$$

to facilitate the tuning process. The best-guess estimates for ϕ , denoted by $\hat{\phi}$, were selected as follows

$$\hat{\phi} = [4 \quad 0.2 \quad 0.25 \quad 5.0 \quad 1.1]^T.$$

The resulting performance of the controller is described by Figures 2-4.

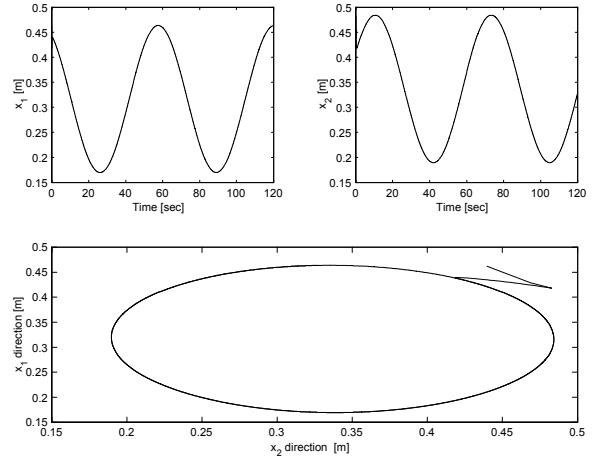


Fig. 2. Actual task-space end-effector trajectory

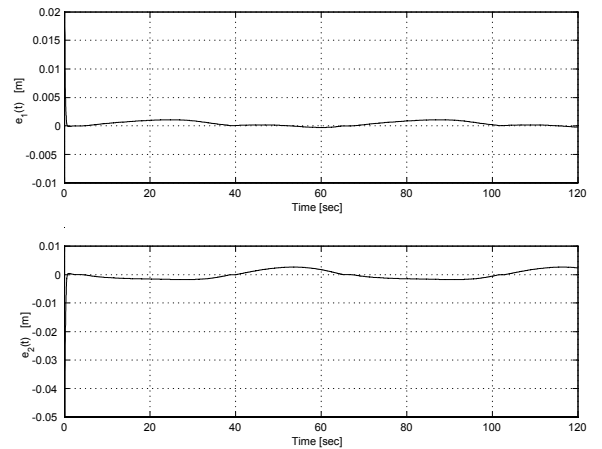


Fig. 3. Task-space tracking errors

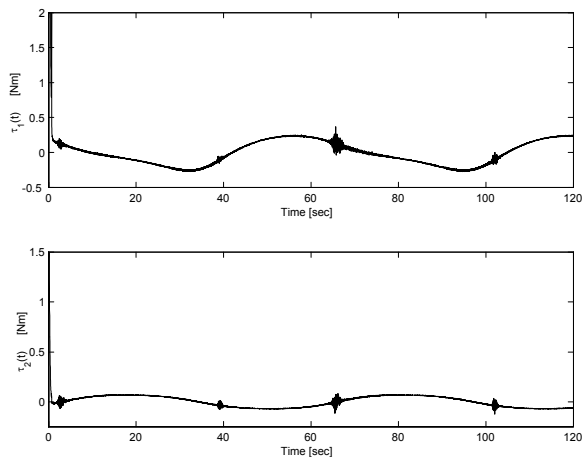


Fig. 4. Control torque inputs to the link actuators

VI. CONCLUSION

In this paper, we proved that the end-effector of a robot manipulator can achieve UUB tracking of an object despite the facts that the object's task-space trajectory is not directly measurable due to parametric uncertainty in the camera calibration parameters (i.e., the relationship between the image-space and the task-space contains parametric uncertainty), and the object motion model and that parametric uncertainty exists in the dynamic model of the robot manipulator. To address the relative velocity issue that is present when an uncalibrated camera-in-hand configuration is utilized, we utilized an interesting cooperative camera configuration and exploited an object motion model to eliminate the need for image-space acceleration measurements. The main advantages of this approach are that: (i) an uncalibrated fixed camera can be mounted to enable a large field-of-view, (ii) the fixed camera can provide relative velocity information (between the object and the end-effector) to the controller, and (iii) an uncalibrated camera-in-hand can be utilized to provide close-up, high resolution information about the object's motion. Future work will target investigating potential advantages of other cooperative camera configurations and demonstrating the performance of the proposed controller in real-time using a high-speed (e.g., capable of capturing 955 frames per second) camera/robot testbed.

REFERENCES

- [1] P. K. Allen, A. Timcenko, B. Yoshimi, and P. Michelman, "Hand-eye coordination for robotic tracking and grasping", In K. Hashimoto, editor, *Visual Servoing*, pp. 33-69, World Scientific Press, 1993.
- [2] R. Andersson, "Real Time Expert System to Control a Robot Ping-Pong Player", Ph.D. thesis, University of Pennsylvania, June 1987.
- [3] B.E. Bishop and M.W. Spong, "Adaptive Calibration and Control of 2D Monocular Visual Servo System", *IFAC Symp. Robot Control*, pp. 525-530, Nantes, France, 1997.
- [4] P. I. Corke and M. C. Good, "Dynamic Effects in Visual Closed-Loop Systems", *IEEE Transactions on Robotics and Automation*, Vol. 12, No. 5, pp. 671-683, October 1996.
- [5] D.M. Dawson, J. Hu, and T.C. Burg, *Nonlinear Control of Electric Machinery*, New York, NY: Marcel Dekker, 1998.
- [6] D.M. Dawson, M.M. Bridges, and Z. Qu, *Nonlinear Control of Robotic Manipulators for Environmental Waste and Restoration*, Englewood Cliffs, NJ: Prentice Hall, 1995.
- [7] *Direct Drive Manipulator Research and Development Package Operations Manual*, Integrated Motion Inc., Berkeley, CA, 1992.
- [8] G. Flandin, F. Chaumette, and E. Marchand, "Eye-in-hand/Eye-to-hand Cooperation for Visual Servoing", *Proc. of the International Conference on Robotics and Automation*, pp. 2741-2746, 2000.
- [9] B. K. Ghosh, N. Xi, T. J. Tarn, *Control in Robotics and Automation: Sensor-Based Integration*, San Diego, CA: Academic Press, 1999.
- [10] G.D. Hager and S. Hutchinson (guest editors), Special Section on Vision-Based Control of Robot Manipulators, *IEEE Trans. Robotics and Automation*, Vol. 12, No. 5, Oct. 1996.
- [11] G.D. Hager, W.C. Chang, and A.S. Morse, "Robot Hand-Eye Coordination Based on Stereo Vision", *IEEE Control Systems Mag.*, Vol. 15, No. 1, pp. 30-39, Feb. 1995.
- [12] G. D. Hagar and Z. Dodds, "A Projective Framework for Constructing Accurate Hand-eye Systems", *Workshop on New Trends in Image Based Robot Servoing in Proc. of the IEEE/RJS International Conference on Intelligent Robots and Systems*, pp. 71-82, 1997.
- [13] N. Hollinghurst and R. Cipolla, "Uncalibrated Stereo Hand-Eye Coordination", *Image and Vision Computing*, Vol. 12, No. 3, pp. 187-192, 1994.
- [14] R. Horaud, F. Dornaika, and B. Espiau, "Visually Guided Object Grasping", *IEEE Transactions on Robotics and Automation*, Vol. 14, No. 4, pp. 525-533, 1998.
- [15] R. Kelly, "Robust Asymptotically Stable Visual Servoing of Planar Robots", *IEEE Trans. Robotics and Automation*, Vol. 12, No. 5, pp. 759-766, Oct. 1996.
- [16] R. Kelly, R. Carelli, O. Nasisi, B. Kuchen, F. Reyes, "Stable Visual Servoing of Camera-in-Hand Robotic Systems", *IEEE Trans. on Mechatronics*, Vol. 5, No. 1, pp. 39-48, March 2000.
- [17] R. Kelly and A. Marquez, "Fixed-Eye Direct Visual Feedback Control of Planar Robots", *J. Systems Engineering*, Vol. 4, No. 5, pp. 239-248, Nov. 1995.
- [18] R. Kelly, F. Reyes, J. Moreno, and S. Hutchinson, "A Two-Loops Direct Visual Control of Direct-Drive Planar Robots with Moving Target", *Proceedings of the IEEE International Conference on Robotics and Automation*, pp. 599-604, 1999.
- [19] R. Kelly, P. Shirkey, and M. Spong, "Fixed-Camera Visual Servo Control for Planar Robots", *Proc. IEEE Conf. Robotics and Automation*, pp. 2643-2649, Minneapolis, MN, Apr. 1996.
- [20] M. Krstic, I. Kanellakopoulos, P. Kokotovic, *Nonlinear and Adaptive Control Design*, New York: John Wiley and Sons, Inc., 1995.
- [21] R.K. Lenz and R.Y. Tsai, "Techniques for Calibration of the Scale Factor and Image Center for High Accuracy 3-D Machine Vision Metrology", *IEEE Trans. Pattern Analysis and Machine Intelligence*, Vol. 10, No. 5, Sept. 1988.
- [22] F.L. Lewis, C.T. Abdallah, and D.M. Dawson, *Control of Robot Manipulators*, New York, NY: MacMillan, 1993.
- [23] N. Maru, S. Y. H. Kase, A. Nishikawa, and F. Miyazaki, "Manipulator Control By Visual Servoing with the Stearo Vision", *Proc. of the IEEE/RJS International Conference on Intelligent Robots and Systems*, pp. 1866-1870, 1993.
- [24] A. Maruyama and M. Fujita, "Robust Visual Servo Control for Planar Manipulators with Eye-In-Hand Configurations", *Proc. Conf. Decision and Control*, pp. 2551-2552, San Diego, CA, Dec. 1997.
- [25] F. Miyazaki and Y. Masutani, "Robustness of Sensory Feedback Control Based on Imperfect Jacobian", *Robotics Research: The Fifth Int. Symp.*, pp. 201-208, H. Miura and S. Arimoto, Eds., Cambridge, MA: MIT Press, 1990.
- [26] B. Nelson and N. Papanikolopoulos (guest editors), Special Issue of Visual Servoing, *IEEE Robotics and Automation Mag.*, Vol. 5, No. 4, Dec. 1998.
- [27] J.J. Slotine and W. Li, *Applied Nonlinear Control*, Englewood Cliff, NJ: Prentice Hall, 1991.
- [28] M.W. Spong and M. Vidyasagar, *Robot Dynamics and Control*, New York, NY: John Wiley and Sons, 1989.
- [29] J. Stavnitzky and D. Capson, "Multiple Camera Model-Based 3-D Visual Servo", *IEEE Transactions on Robotics and Automation*, Vol. 16, No. 6, Dec. 2000.
- [30] M. Takegaki and S. Arimoto, "A new feedback method for dynamic control of manipulators", *Transactions of ASME Journal of Dynamical Systems, Measurement, and Control*, vol. 103, pp. 119-125, June 1981.
- [31] E. Zergeroglu, D.M. Dawson, M.S. de Queiroz, and A. Behal, "Vision-Based Nonlinear Tracking Controllers with Uncertain Robot-Camera Parameters", *Proceedings of the IEEE/ASME International Conference on Advanced Methatronics*, pp. 854-859, 1999. Also accepted to appear in *IEEE/ASME Trans. on Mechatronics*, Vol. 6, No 3, September 2001.
- [32] E. Zergeroglu, D. M. Dawson, M. de Queiroz, and S. Nagarkatti, "Robust Visual-Servo Control of Planar Robot Manipulators in the Presence of Uncertainty", *Proc. of the 38th IEEE Conference on Decision and Control*, pp. 4137-4142, 1999.